3B2v8.06a/w (Dec 5 2003).51c + model | JBMT : 5106 | Prod.Type:FTP pp.1–8(col.fig.:1–2,4–6) | ED:MadhupRaj PAGN:Mishra SCAN:

ARTICLE IN PRESS

Available online at www.sciencedirect.com

SCIENCE DIRECT

ELSEVIER

Biomaterials ▮ (▮▮▮▮) ▮▮▮–▮▮▮

Biomaterials

www.elsevier.com/locate/biomaterials

# Mesoporous carbide-derived carbon with porosity tuned for efficient adsorption of cytokines

Gleb Yushin[a], Elizabeth N. Hoffman[a], Michel W. Barsoum[a], Yury Gogotsi[a,*], Carol A. Howell[b], Susan R. Sandeman[b], Gary J. Phillips[b], Andrew W. Lloyd[b], Sergey V. Mikhalovsky[b]

[a]*Department of Materials Science and Engineering and A.J. Drexel Nanotechnology Institute, Drexel University, Philadelphia, PA 19104, USA*
[b]*School of Pharmacy and Biomolecular Sciences, University of Brighton, Moulsecoomb, Brighton BN2 4GJ, UK*

Received 31 May 2006; accepted 17 July 2006

**Abstract**

Porous carbons can be used for the purification of various bio-fluids, including the cleansing blood of inflammatory mediators in conditions such as sepsis or auto-immune diseases. Here we show that the control of pore size in carbons is a key factor to achieving efficient removal of cytokines. In particular, the surface area accessible by the protein governs the rate and effectiveness of the adsorption process. We demonstrate that novel mesoporous carbon materials synthesized from ternary MAX-phase carbides can be optimized for efficient adsorption of large inflammatory proteins. The synthesized carbons, having tunable pore size with a large volume of slit-shaped mesopores, outperformed all other materials or methods in terms of efficiency of TNF-α removal and the results are comparable only with highly specific antibody–antigen interactions.


*Keywords:* Carbon; Protein adsorption; Adsorption; Cytokine

## 1. Introduction

The worldwide occurrence of sepsis with over 18 million cases recorded annually and the absence of efficient drug-based therapies, make this systemic inflammatory response to infection one of the leading causes of death [1]. Severe sepsis, which accounts for over 17% of the total sepsis cases, and having a current mortality rate 30–40%, is responsible for the death of 1500 people/day worldwide, on a scale comparable to lung and breast cancer (~2700 and ~1100 people /day, respectively) [1,2]. From an economic perspective, sepsis places a significant burden on healthcare systems, costing over $17 billion/year in the US alone [3]. The inflammatory response to various bodily insults is driven by a complex network of inflammatory mediators; these consist mainly of proteins called cytokines [4–6]. Cytokine removal from blood may help to bring under control the unregulated pro- and anti-inflammatory processes driving sepsis. Therapies aimed at the simultaneous reduction of cytokines across a wide range of molecular sizes might, therefore, prove more effective than drugs directed against a single or a few inflammatory mediators [5–7]. Hemofiltration or hemoadsorption could allow extracorporeal removal of these inflammatory cytokines to an extent that is sufficient to strongly reduce the inflammatory response. While both sieving and adsorption could play a role in hemofiltration, the adsorption characteristics of the filter material are generally believed to be a dominant factor in membrane efficiency. Adsorption can remove toxins without introducing other substances into the blood. Therefore, hemoadsorption might have advantages over hemofiltration, having the same or better efficiency in the treatment of inflammatory diseases, being of lower cost and offering considerably better comfort for patients during and after the treatments [8].

*Corresponding author. Tel.: +1 215 895 6211.
*E-mail address:* gogotsi@drexel.edu (Y. Gogotsi).

0142-9612/$ - see front matter © 2006 Elsevier Ltd. All rights reserved.
doi:10.1016/j.biomaterials.2006.07.019

Activated carbons (ACs), known for over 3000 years, still remain the most powerful conventional adsorbents [8], mainly due to their highly developed porous structure and large surface area. Most of the specially purified ACs prepared from synthetic polymers show excellent biocompatibility and do not require special coatings for direct contact with blood [8,9]. However, despite extensive studies and improvements in the activation processes, little control over the pore structure has been achieved. Even advanced ACs show limited performance in adsorbing large inflammatory proteins, mostly due to the limited surface area accessible to the adsorbate. Templating has previously been used to increase the volume fraction of the larger pores [10–12]. For example, porous carbon was prepared by introducing carbon into the pores of alumina or silica substrates and subsequently dissolving the oxide template by acidic treatment. Apart from cost issues, the resulting carbon generally demonstrates poor mechanical integrity and near-spherical shape of the pores with the bottlenecks that do not allow large molecules to be adsorbed inside the bulk of the particles. In principle, it follows that interconnected slit-shaped pores of an optimized size would be more advantageous for the discussed application. Small particles (<100 nm) would offer a larger external surface, but they cannot be used in most of the biomedical applications due to difficulties of filtering them from the biofluids. The pore size in other porous carbon materials, such as carbon nanotubes (CNT), is very difficult to control and tune to the desired values. Most CNTs have a low specific surface area (SSA) and agglomeration of CNT into ropes, particularly when they are brought in contact with biofluids, generally significantly reduces their accessible surface area.

Carbon produced by etching of metal(s) from metal carbides and called carbide derived carbon (CDC) has recently been shown to offer great potential for controlling the size of micropores (0.4–2 nm) [13]. CDCs are generally produced by chlorination of carbides in the 200–1200 °C temperature range. Metals and metalloids are removed as chlorides, leaving behind a collapsed noncrystalline carbon with up to 80% open pore volume. The detailed nature of the porosity—average size and size distribution, shape, and total SSA—can be tuned with high sensitivity by the judicious selection of the precursor carbide (composition, lattice type, etc.) [13–16] and chlorination temperature [13]. However, only tuning of microporosity (0.4–2 nm) has been demonstrated in CDCs so far. In this paper, we demonstrated a method to produce porous carbons with controlled volume and surface area of slit-shaped mesopores (2–50 nm) of certain size by CDC synthesis from selected ternary (MAX-phase) carbides [17] and investigated the effect of pore structure on removal of cytokines from blood.

## 2. Materials and methods

### 2.1. Materials

CDCs were synthesized from $Ti_2AlC$ and $Ti_3AlC_2$ powders by the reaction with pure chlorine (99.5%, BOC gases) at 600, 800 and 1200 °C. Both carbides were produced at Drexel University, but are now commercially available (3-ONE-2, Inc, NJ, US). They belong to the MAX-phase group of ternary carbides, having a layered hexagonal structure with carbon atoms positioned in basal planes and separated by 0.68 nm ($Ti_2AlC$) or alternating layers of 0.31 and 0.67 nm ($Ti_3AlC_2$) [18]. The CDCs produced from these carbides are known to possess slit-shaped open pores [13,19,20]. The average particle size of the carbide samples used in our experiments was ~10 μm, as measured using a particle size analyzer (Horiba LA-910, Japan). For CDC synthesis, the selected carbide powder was placed onto a quartz sample holder and loaded into the hot zone of a horizontal quartz tube furnace. Prior to heating, the tube (~30 mm in diameter) was purged with high purity Ar (BOC Gases, 99.998%) for 30 min at a flow rate of 100 sccm. Once the desired temperature was reached and stabilized, the Ar flow was stopped and a 3-h chlorination began with $Cl_2$ flowing at a rate of 10 sccm. After the completion of the chlorination process, the samples were cooled down under a flow of Ar (40 sccm) for about 5 h to remove any residual chlorine or metal chlorides from the pores, and taken out for further analyses. In order to avoid a back-stream of air, the exhaust tube was connected to a bubbler filled with sulfuric acid. A detailed description of the chlorination apparatus used in this study can be found elsewhere [21].

The sorption performance of the CDCs was compared with that of Adsorba 300C and CXV carbon adsorbents. Adsorba 300C is an activated carbon produced by Norit from peat, and coated with a 3–5 μm thick cellulose membrane for better hemocompatibility. It is commercially used in adsorbent-assisted extracorporeal systems manufactured by Gambro, Sweden. CXV is an AC obtained from CECA (subsidiary of Arkema, France), known to be extremely efficient for cytokine removal applications and thus used as a benchmark reference.

### 2.2. Characterization

The structure of the CDCs was investigated using high-resolution transmission electron microscopy (HRTEM). The TEM samples were prepared by 2 min sonication of the CDC powder in isopropanol and deposition on the lacey-carbon coated copper grid (200 mesh). A field-emission TEM (JEOL 2010F, Japan) with an imaging filter (Gatan GIF) was used at 200 kV.

The porosity of CDCs was studied using automated micropore gas analyzers Autosorb-1 and Nova (Quantachrome Instruments, USA). The $N_2$ and Ar sorption isotherms were obtained at liquid nitrogen temperature (−196 °C) in the relative pressure $P/P_0$ range of about $8\times10^{-7}$–1 and $2\times10^{-2}$–1, respectively. The isotherms were analyzed using Brunauer–Emmet–Teller (BET) equation and non-local density functional theory (NLDFT) [22–25] to reveal the SSA and pore-size distributions (PSD) of the CDCs. The SSAs calculated using BET and DFT theory are referred to as BET–SSA and DFT–SSA, respectively. A difference in absolute values between BET–SSA and DFT–SSA is expected, as both types of calculations are based on different assumptions, which might not be justified with the utmost accuracy for all the materials under study. Quantachrome Instruments data reduction software Autosorb v.1.50 [22] was employed for the porosity analysis. Slit-shaped pores were assumed for the calculations.

### 2.3. Cytokine adsorption experiments

Fresh frozen human plasma (NBS, UK) was defrosted and spiked with the recombinant human cytokines (TNF-α, IL-1β, IL-6, and IL-8; all obtained from BD Biosciences, USA) at a concentration of about 1000, 500, 5000 and 500 pg/ml, respectively. These levels are comparable with

the concentrations measured in the plasma of patients with sepsis [26–28]. Carbon adsorbents (0.02 g) were equilibrated in phosphate-buffered saline (PBS) (0.5 ml) overnight prior to removal of PBS and addition of 800 μl of spiked human plasma. Controls consisted of spiked plasma with no adsorbent present. Adsorbents were incubated at 37 °C while shaking (90 rpm). At 5, 30 and 60 min time points, samples were centrifuged (125 g) and the supernatant collected and stored at −20 °C prior to ELISA (BD Biosciences) analysis for the presence of cytokines. Samples were diluted 1:4 (TNF-α, IL-8, IL-1β) and 1:10 (IL-6) in assay diluent prior to analysis.

## 3. Results and discussion

### 3.1. Porosity characterization

Fig. 1 shows the $N_2$ sorption isotherms of CDCs (Fig. 1A) and commercial carbon samples (Fig. 1B). All the samples, except Adsorba 300C, demonstrate type IV isotherm according to the Brunauer classification [24] with a characteristic hysteresis, suggesting the presence of mesopores (pores with size in the 2–50 nm range). CDCs from both $Ti_2AlC$ (Fig. 1A) and $Ti_3AlC_2$ (not shown) demonstrate similar trends as the temperature of synthesis changes. The volume of $N_2$ adsorbed in the porous structure of CDC prepared at lower temperature (600 °C) approaches half of the maximum values at low relative pressure ($P/P_0$). The steep slope of the adsorption curve at $P/P_0$ values approaching 1, associated with capillary condensation in mesopores, is quite short, suggesting a small mesopore volume [22]. The $N_2$ sorption behavior changes dramatically at intermediate (~800 °C) chlorination temperatures. The total volume of adsorbed $N_2$ more than doubles; an increase is observed over the whole $P/P_0$ range, indicating a significant increase in both the total and mesopore volume. The level of adsorption–desorption hysteresis, and the steep slope as $P/P_0$ approaches unity also increases substantially, in agreement with the suggested increase in the relative volume of mesopores. As the synthesis temperature increases to 1200 °C, the volume of adsorbed $N_2$ further increases in the $P/P_0$ range of up to ~0.8, but becomes lower at higher $P/P_0$ values (Fig. 1A). Such changes in the isotherm shape indicate the reduction in the relative volume of larger mesopores.

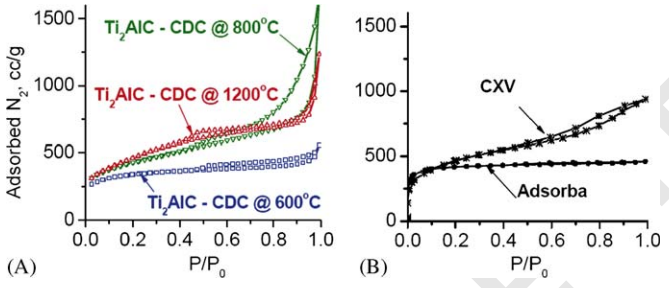


Fig. 1. Nitrogen sorption isotherms. (A) $Ti_2AlC$ CDC, (B) CXV and Adsorba samples. $N_2$ isotherms for $Ti_3AlC_2$ CDC are very similar to the isotherms for $Ti_2AlC$ CDC synthesized at identical temperatures.

The PSD curves calculated in the 1.5–36 nm range for all the studied samples from the $N_2$ isotherms (Fig. 2) fully support the aforementioned conclusions. The CDC samples formed at low temperature (600 °C) have a very low volume of mesopores, particularly those above 10 nm (Figs. 2B and F). At the intermediate synthesis temperatures (800 °C), the PSD becomes wider and shifts to higher pore-size values (Figs. 2C and G). These samples clearly have the largest volume of mesopores above 5 nm. At the high chlorination temperature of 1200 °C the total CDC mesopore volume remains relatively high (Figs. 2D and H). It is in fact higher than the total pore volume of many activated carbon samples, including Adsorba 300C (Fig. 2A). However, most of the mesopores in these samples are below 4–5 nm. Adsorba 300C has the smallest volume of mesopores and is almost purely microporous carbon. The PSD of the CXV sample (Fig. 2E) is close to that of an average of CDC samples produced at high and intermediate temperatures. The porosity data for all the studied samples are summarized in Table S1 (Supplementary Information).

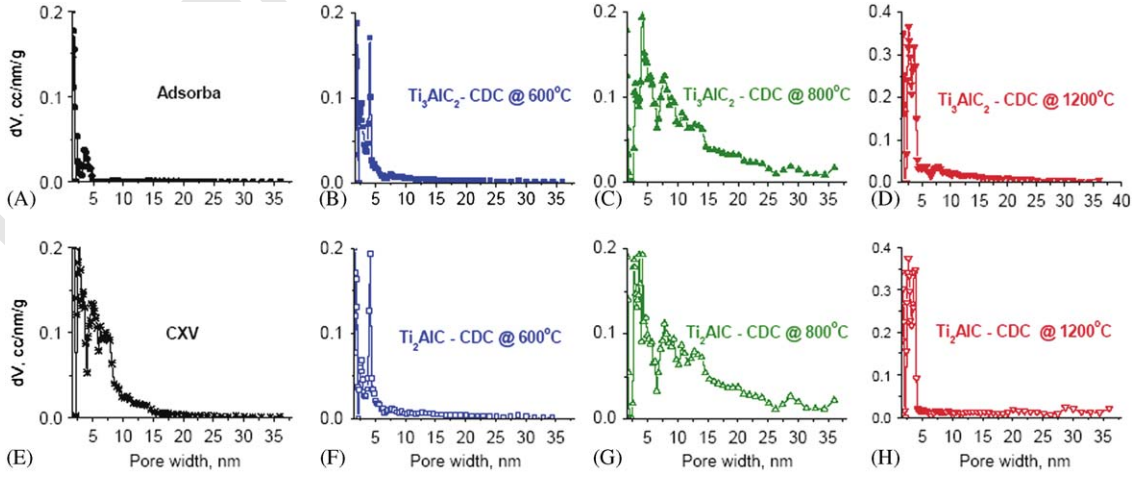


Fig. 2. Distribution of pore sizes of porous carbons in the 1.5–36 nm range obtained from $N_2$ sorption isotherms. (A) Adsorba, (B–D) CDC produced from $Ti_3AlC_2$ at 600, 800, and 1200 °C, (E) CXV, (F–H) CDC produced from $Ti_2AlC$ at 600, 800, and 1200 °C.

While Ar sorption is not a very efficient technique to study the large mesopores, it gives more accurate PSD results for small (<4 nm) pore values, mainly due to argon's smaller atomic size, the absence of quadrupole moment (which can potentially lead to localized adsorption as in case of $N_2$) and its weaker interactions with carbon adsorbents. The PSD of the studied samples in the 0.4–4-nm range obtained from Ar sorption isotherms (Supplementary Information, Fig. S1) revealed details of the samples' microporosity. Similar to Adsorba 300C, both CDC samples produced at 600 °C have the majority of pores below 2 nm in width. As the CDC synthesis temperature increases, the average size of the pores in the 0.4–4-nm range increases as well (Fig. S1). However, above 800 °C, pores in the 2–4-nm range have a tendency to grow on the account of the micropores, forming a large volume of ~3 nm pores at 1200 °C. The PSD of the CXV sample is close to the average between the CDC samples formed at 800 and 1200 °C.

### 3.2. Transmission electron microscopy

TEM revealed disordered microstructure of all the studied carbons. The degree of disorder was different between the carbons. Both CDCs formed at 600 °C demonstrate completely amorphous structure, without any graphite fringes visible (Fig. 3A). Increasing the CDC-processing temperature to 800 °C resulted in the formation of short-curved graphene structures, considered turbostratic carbon (Fig. 3B). At 1200 °C TEM detected markedly increased ordering and the formation of long and thin (1–3 graphene sheets) graphite ribbons (Fig. 3C). At the edge of the particles, ribbons with up to 10 graphene layers were found (Fig. 3C). The microstructure of Adsorba 300C sample was found to be highly amorphous, (Fig. 3D) while that of the CXV carbon (Fig. 3E), turbostratic.

Our previous studies have shown that the observed evolution of ordering within the carbon structure with the chlorination temperature is quite common for most of the CDCs obtained from both ternary and binary carbides [21]. The changes in the PSDs correlate to changes in the CDC microstructure. The low mobility of the carbon atoms at the low chlorination temperatures resulted in the formation of a uniform amorphous structure (Fig. 3A) with small micropores (Figs. 2B and F; Figs. S1B, S1F). At higher synthesis temperatures, higher carbon mobility allowed for the formation of graphitic ribbon networks (Fig. 3C), with mesopores forming between the graphene ribbons and micropores in the imperfections of the graphitic ribbons or within the remaining disordered carbon (Figs. 2D and H; Figs. S1D, S1H). At the intermediate temperature of 800 °C, the mobility of carbon was high enough to allow for a redistribution of carbon atoms into defective graphene sheets and the collapse of several sheets into stacks forming mesopores between them. However, the mobility was still too low to allow uniform linking between the turbostratic ribbons, resulting in a wide distribution of mesopores (Figs. 2C and G). Note, that since precise determination of non-spherical pores in disordered non-planar particles is not possible using TEM, we relied on gas sorption measurements for the PSD determination.

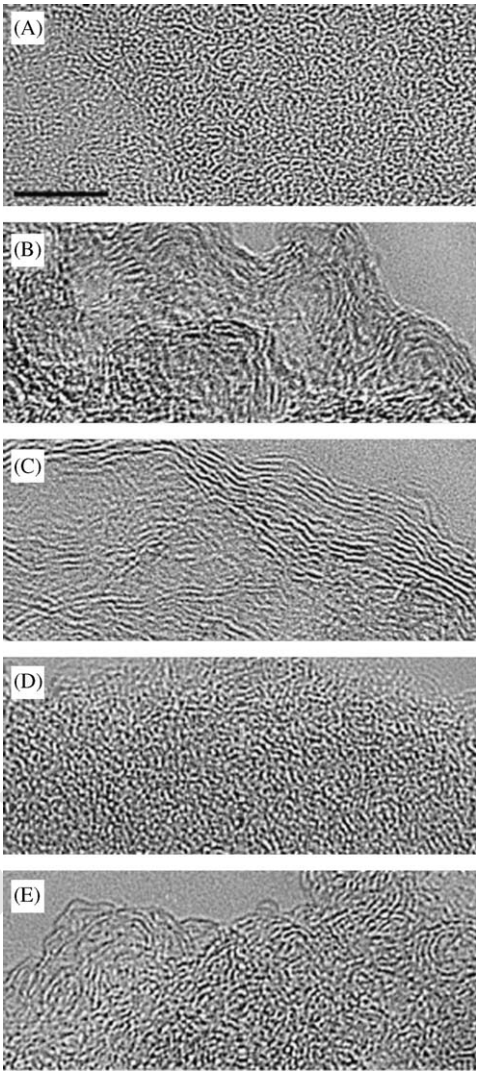


Fig. 3. Transmission electron microscopy of porous carbon samples. (A–C) CDC produced from $Ti_2AlC$ at 600, 800 and 1200 °C, (D) Adsorba, (E) CXV. The structure of $Ti_3AlC_2$ CDC replicates the one for $Ti_2AlC$ CDC if synthesized at identical temperatures. Scale bar = 5 nm.

### 3.3. Cytokine adsorption

Fig. 4 compares efficiency of removal of two selected cytokines (tumor necrosis factor alpha (TNF-α) and interleukin-6 (IL-6)) from human plasma using the investigated carbons. Adsorption of TNF-α is known to be the most challenging task, probably due to a large size (> 9.4 nm) of the trimeric (most common) form of this cytokine [29]. Adsorba 300C and CDC produced at 600 °C, which have small pores, did not noticeably change the protein concentration over time. CDC produced at 1200 °C and CXV also demonstrated a limited success in the

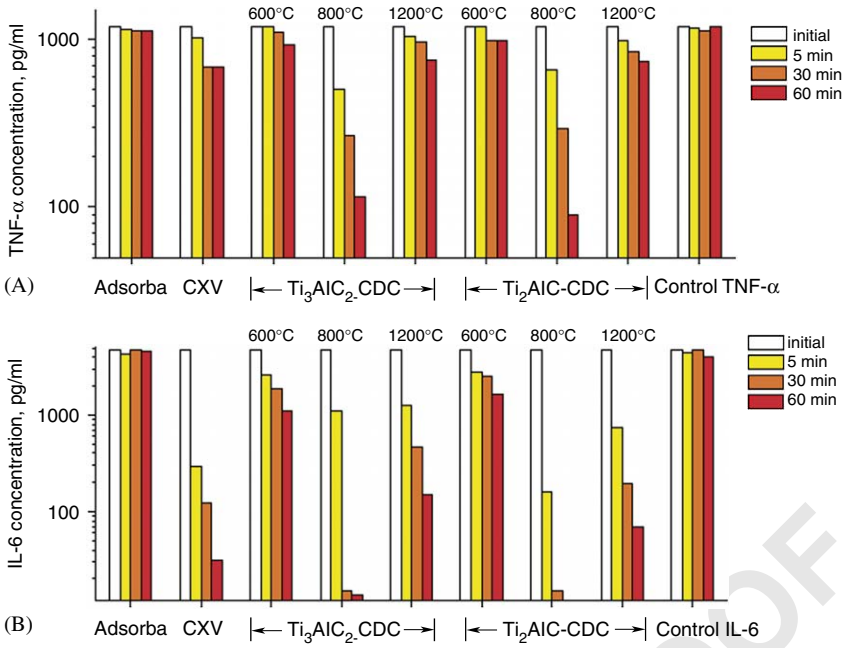


Fig. 4. Comparison of the porous carbons efficiency in the cytokine removal from human blood plasma. (A) Concentration of TNF-α in the plasma solution initially and after 5, 30 and 60 min of adsorption. (B) Similar changes in IL-6 concentration. Both CDC samples produced at 800 °C and having developed mesoporosity outperformed other materials in the efficiency of cytokines removal.

adsorption of TNF-α, decreasing its concentration by about 40% after 1 h of adsorption (Fig. 4A), similar to that observed in advanced porous carbon hemoadsorption systems [30]. In contrast, both CDC samples prepared at 800 °C decreased the protein concentration by over 13 times in this time period. To the best of our knowledge, in these experiments CDCs outperformed any other material or method for the efficient removal of TNF-α, and the results are comparable only to highly specific antibody–antigen interactions [31,32].

Adsorption of the smaller cytokine IL-6 by most of the studied carbons was noticeably higher, but demonstrated similar trends (Fig. 4B). Strictly microporous Adsorba 300C was clearly inefficient. However, CDCs prepared at 600 °C, having a limited amount of mesopores (pores 2–50 nm), adsorbed 66–77% of the cytokines initially present in the solution in 1 h. The CDCs produced at 1200 °C demonstrated 97–98.5% adsorption, which is comparable to the CXV sample, capable of adsorbing ~99%. The CDCs prepared from $Ti_2AlC$ at 800 °C, having the most developed mesoporosity decreased IL-6 concentration by ~99.8%; the remaining IL-6 was close to the detection limit of the ELISA used.

A clear dependence of protein removal efficiency on the PSDs of the porous carbons is seen when protein adsorption is plotted as a function of the carbons' accessible surface area, which is approximated as the SSA of pores exceeding the smallest protein dimension in size (Fig. 5). Dimensions of the investigated cytokines were considered to be: $9.4 \times 9.4 \times 11.7$ nm (trimer of TNF-α) [29], $5.5 \times 5.5 \times 7.7$ nm (IL-1$\beta$) [33], $5 \times 5 \times 12.2$ nm (IL-6) [34], $4 \times 4 \times 9$ nm (IL-8) [35]. The larger the surface areas of the porous carbons accessible to a given cytokine ($SSA_{acc}$), the more cytokines were adsorbed at a given time (Figs. 5A–D). Some scattering in the results obtained could be explained by experimental errors in the estimation of the cytokine concentration and the carbon PSD. Depending on the cytokine and its initial concentration, values of the $SSA_{acc}$ above 50–100 $m^2/g$ were generally sufficient for fast and efficient cytokine removal. The relatively short and small IL-1$\beta$ and IL-8 cytokines diffused so rapidly into the carbon pores that 5 min was sufficient to adsorb most of these proteins by carbons with $SSA_{acc}$ exceeding 50 $m^2/g$ (Figs. 5B and D). The existence of larger channels within these carbons should have further accelerated the adsorption process. IL-6 demonstrated slower adsorption (Fig. 5C), probably due to its longer dimensions and hence slower diffusion within the carbon pore structure. The TNF-α trimer, the largest adsorbate, demonstrated a further decrease in adsorption rate (Fig. 5A) as the amount of pores, exceeding three times the adsorbate size needed for fast diffusion, was limited (Figs. 2C and G).

Historically, in medical sciences and applied medicine, ACs are considered to be high SSA carbons of ultra purity. Differentiation of ACs with respect to difference in their PSD is uncommon. In fact, the same carbon materials are often used for adsorption of various species, from gases to organic molecules. However, since most commercial medical grade ACs, including Adsorba, are primarily microporous (Figs. 2A, Fig. S1A), adsorption of inflammatory mediators with size exceeding 2 nm could only take place on the particles' surface (Fig. 6A). The calculated SSA of spherical carbon particles with a 10 μm diameter and 50% porosity is only ~0.3 $m^2/g$, which is much smaller

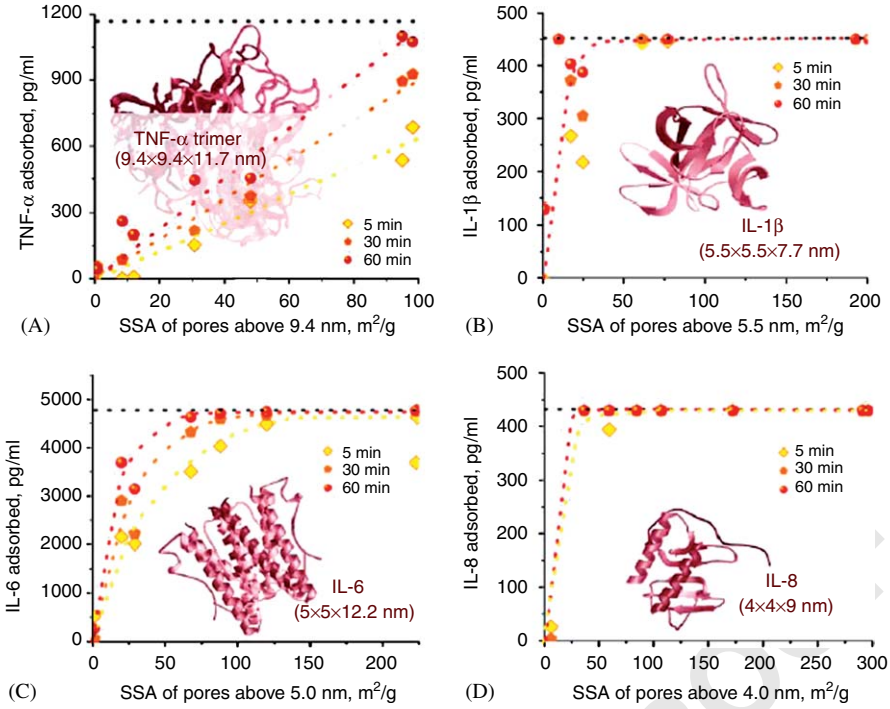


Fig. 5. Adsorption of cytokines by porous carbons as a function of the surface area accessible to the cytokines. (A) TNF-α, (B) IL-1β, (C) IL-6, (D) IL-8. The accessible area is approximated as the SSA of pores exceeding the smallest protein dimension in size: 9.4 nm for TNF-α trimer, 5.5 nm for IL-1β, 5 nm for IL-6, and 4 nm for IL-8. Amount of the adsorbed cytokines was measured after 5, 30 and 60 min adsorption. Larger carbon surface area accessible to the cytokines clearly results in faster and more complete adsorption. The horizontal dotted black line on the top of each graph indicates the initial concentration of the cytokines in plasma.

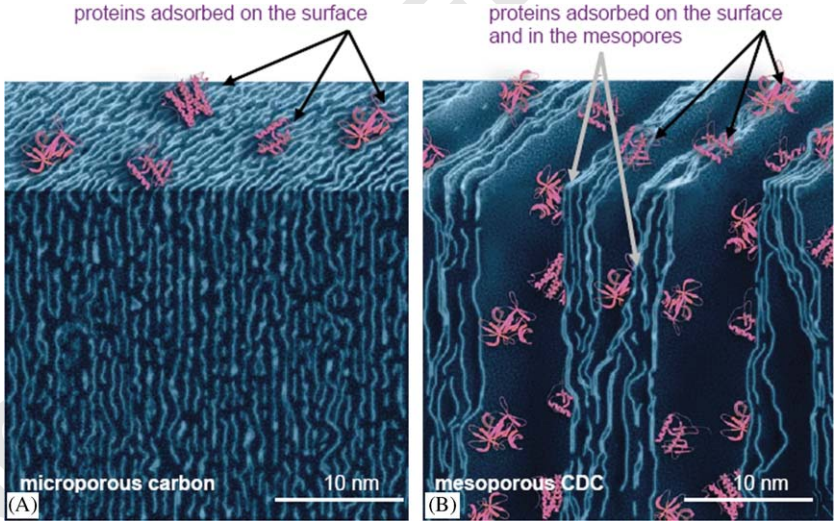


Fig. 6. Schematics of protein adsorption by porous carbons. (A) Surface adsorption in microporous carbon. Small pores do not allow proteins (shown in pink) to be adsorbed in the bulk of carbon particles (shown in blue). (B) Adsorption in the bulk of mesoroporous CDC. Large mesopores are capable to accommodate most of the proteins. Carbon particles are shown in cross-section. Alignment of the slit-shaped pores drawn in both illustrations is a simplification.

than the 386–406 $m^2/g$ SSA of mesopores (2–50 nm) in the CDCs produced at 800 °C. It is thus not too surprising that clinical trials of commercial extracorporeal adsorption systems did not show significantly decreased mortality in patients with sepsis [36,37]. Large biological molecules can move through pores of appropriate size, as translocation of DNA through a nanotube demonstrated recently [38], and be adsorbed in the bulk of the adsorbent particles (Fig. 6B). Pore size control is thus a key issue for achieving highly efficient removal of large cytokines from blood plasma. Engineering of novel nanostructured CDC adsorbents, with rationally optimized porosity may provide a

solution for extracorporeal adsorption systems and save the lives of people suffering severe sepsis. Similar approaches could be used for the selective adsorption of other large organic molecules and possibly viruses for other bio-related or medical applications.

## 4. Conclusions

Chlorination of layered ternary MAX-phase carbides has made it possible to synthesize mesoporous carbons with large-surface areas and volumes of slit-shaped mesopores. Based on this work it appears that not only micropores (0.4–2 nm) but also mesopores (2–50 nm) can be tuned in a controlled way by extraction of metals from carbides, providing a mechanism for the optimization of adsorption systems for selective sorption of a large variety of biomolecules.

## Acknowledgements

This research was supported by the US National Science Foundation. TEM studies were performed at Penn Regional Nanotechnology Facility, University of Pennsylvania. Additional material characterization was performed at the Centralized Materials Characterization Facility of the A.J. Drexel Nanotechnology Institute. E. N. Hoffman was supported by the NSF IGERT Grant # DGE-0221664.

## Appendix A. Supplementary data

Supplementary data associated with this article can be found in the online version at doi:10.1016/j.biomaterials.2006.07.019.

## Reference

[1] Slade E, Tamber PS, Vincent JL. The surviving sepsis campaign: raising awareness to reduce mortality. Crit Care 2003;7(1):1–2.
[2] Williams MD, Braun LA, Cooper LM, Johnston J, Weiss RV, Qualy RL, et al. Hospitalized cancer patients with severe sepsis: analysis of incidence, mortality, and associated costs of care. Crit Care 2004;8(5):R291–8.
[3] Angus DC, Linde-Zwirble WT, Lidicker J, Clermont G, Carcillo J, Pinsky MR. Epidemiology of severe sepsis in the United States: Analysis of incidence, outcome, and associated costs of care. Crit Care Med 2001;29(7):1303–10.
[4] Asachenkov A, Marchuk G, Mohler R, Zuev S. Immunology and disease control: a system approach. IEEE Trans Biomed Eng 1994;41:943–53.
[5] Callard R, George A, Stark J. Cytokines, chaos, and complexity. Immunity 1999;11:507–13.
[6] Neugebauer E, Willy C, Sauerland S. Complexity and non-linearity in shock research: reductionism or synthesis? Shock 2001;16:252–8.
[7] Natanson C, Esposito CJ, Banks SM. The sirens' songs of confirmatory sepsis trials: selection bias and sampling error. Crit Care Med 1998;26:1927–31.
[8] Mikhalovsky SV. Emerging technologies in extracorporeal treatment: Focus on adsorption. Perfusion-UK 2003;16(2):47–54.
[9] Sandeman SR, Howell CA, Phillips GJ, Lloyd AW, Davies JG, Mikhalovsky SV, et al. Assessing the in vitro biocompatibility of a novel carbon device for the treatment of sepsis. Biomaterials 2005;26(34):7124–31.
[10] Ryoo R, Joo SH, Jun S. Synthesis of highly ordered carbon molecular sieves via template-mediated structural transformation. J Phys Chem B 1999;103(37):7743–6.
[11] Xia YD, Mokaya R. Ordered mesoporous carbon hollow spheres nanocast using mesoporous silica via chemical vapor deposition. Adv Mater 2004;16(11):886–91.
[12] Lee J, Han S, Hyeon T. Synthesis of new nanoporous carbon materials using nanostructured silica materials as templates. J Mater Chem 2004;14(4):478–86.
[13] Gogotsi Y, Nikitin A, Ye H, Zhou W, Fischer JE, Yi B, et al. Nanoporous carbide-derived carbon with tunable pore size. Nat Mater 2003;2:591–4.
[14] Dash RK, Yushin G, Gogotsi Y. Nanoporous carbon derived from zirconium carbide. Micropor Mesopor Mater 2005;86:50–7.
[15] Dash RK, Yushin G, Laudisio G, Fischer JE, Gogotsi Y. Titanium carbide-derived nanoporous carbon for energy-related applications. Carbon, 2006.
[16] Dash RK, Nikitin A, Gogotsi Y. Microporous carbon derived from boron carbide. Micropor Mesopor Mater 2004;72:203–8.
[17] Barsoum BM, El-Raghy T. The MAX phases: unique new carbide and nitride materials. Am Sci 2001;89:334–43.
[18] Barsoum MW. The $M_{N+1}AX_N$ phases: a new class of solids. Prog Solid State Chem 2000;28:201–81.
[19] Yushin G, Hoffman E, Nikitin A, Ye H, Barsoum MW, Gogotsi Y. Synthesis of nanoporous carbide-derived carbon by chlorination of titanium silicon carbide. Carbon 2005;44(10):2075–82.
[20] Hoffman E, Yushin GN, Barsoum BM, Gogotsi G. Synthesis of nanoporous carbide-derived carbon by chlorination of titanium aluminum carbide. Chem Mater 2005;17(9):2317–22.
[21] Yushin G, Gogotsi Y, Nikitin A. Carbide derived carbon. In: Gogotsi Y, editor. Nanomaterials handbook. Boca Raton, FL: CRC Press; 2005. p. 239–82.
[22] Ravikovitch PI, Neimark AV. Characterization of nanoporous materials from adsorption and desorption isotherms. Colloids Surf A: Phys Eng Aspects 2001;187–188:11–21.
[23] Brunauer S, Emmett P, Teller E. Adsorption of gases in multimolecular layers. J Am Chem Soc 1938;60:309–19.
[24] Gregg SJ, Sing KSW. Adsorption, Surface Area and Porosity. London: Academic Press; 1982.
[25] Lowell S, Schields JE. Powder surface area and porosity, New York, 1998.
[26] Cohen J, Abraham E. Microbiological findings and correlations with serum tumour necrosis factor alpha in patients with severe septic shock. J Infect Dis 1999;180:116–21.
[27] Heering P, Morgera S, Schmitz FJ, Schmitz G, Willers R, Schultheiss HP, et al. Cytokine removal and cardiovascular hemodynamics in septic patients with continuous venovenous hemofiltration. Int Care Med 1997;23:228–96.
[28] Marum S, Riberio JP, Arranhado E, Lage H, Mota L, Marcelino P, et al. Cytokines and sepsis—just black smoke. Crit Care Med 2000;4:66.
[29] Reed C, Fu ZQ, Wu J, Xue YN, Harrison RW, Chen MJ, et al. Crystal structure of TNF-alpha mutant R31D with greater affinity for receptor R1 compared with R2. Protein Eng 1997;10(10):1101–7.
[30] Kellum JA, Song MC, Venkataraman R. Hemoadsorption removes tumor necrosis factor, interleukin-6, and interleukin-10, reduces nuclear factor-kappa B DNA binding, and improves short-term survival in lethal endotoxemia. Crit Care Med 2004;32(3):801–5.
[31] Weber V, Linsberger I, Ettenauer M, Loth F, Hoyhtya M, Falkenhagen D. Development of specific adsorbents for human tumor necrosis factor-alpha: influence of antibody immobilization on performance and biocompatibility. Biomacromolecules 2005;6(4):1864–70.
[32] Hinterdorfer P, Baumgartner W, Gruber HJ, Schilcher K, Schindler H. Detection and localization of individual antibody-antigen

recognition events by atomic force microscopy. Proc Natl Acad Sci USA 1996;93(8):3477–81.

[33] Einspahr H, Clancy LL, Muchmore SW, Watenpaugh KD, Harris PKW, Carter DB, et al. Crystallization of recombinant human interleukin 1-beta. J Cryst Growth 1988;90(1–3):180–7.

[34] Somers W, Stahl M, Seehra JS. 1.9 angstrom crystal structure of interleukin 6: implications for a novel mode of receptor dimerization and signaling. Embo J 1997;16(5):989–97.

[35] Rajarathnam K, Clarklewis I, Sykes BD. H-1-Nmr solution structure of an active monomeric interleukin-8. Biochemistry 1995;34(40):12983–90.

[36] Reinhart K, Meier-Hellmann A, Beale R, Forst H, Boehm D, Willatts S, et al. Open randomized phase II trial of an extracorporeal endotoxin adsorber in suspected gram-negative sepsis. Crit Care Med 2004;32(8):1662–8.

[37] Cole L, Bellomo R, Hart G, Journois D, Davenport P, Tipping P, et al. A phase II randomized, controlled trial of continuous hemofiltration in sepsis. Crit Care Med 2002;30(1):100–6.

[38] Fan R, Karnik R, Yue M, Li DY, Majumdar A, Yang PD. DNA translocation in inorganic nanotubes. Nano Lett 2005;5(9):1633–7.